iJRASET
International Journal For Research in Applied Science and Engineering Technology

INTERNATIONAL JOURNAL FOR RESEARCH

IN APPLIED SCIENCE & ENGINEERING TECHNOLOGY

Volume: 14 **Issue:** IV **Month of publication:** April 2026

DOI: https://doi.org/10.22214/ijraset.2026.80702

www.ijraset.com

Call: 08813907089 | E-mail ID: ijraset@gmail.com

International Journal for Research in Applied Science & Engineering Technology (IJRASET)
ISSN: 2321-9653; IC Value: 45.98; SJ Impact Factor: 7.538
Volume 14 Issue IV Apr 2026- Available at www.ijraset.com

Power Quality Enhancement in Grid-Connected EV Charging Stations Using SRF-Based Shunt Active Power Filter

Pratik Potdukhe[1], Prof. Praful Tadse[2]
M.Tech Scholar, [2]Professor, Department of Electrical Engineering, BIT – Ballarpur Institute of Technology, Ballarpur, Maharashtra, India

Abstract: ***Contemporary electric vehicle (EV) charging infrastructure heavily relies on nonlinear power electronic converters that inject harmonic currents into the distribution network, significantly deteriorating power quality. This paper addresses the harmonic mitigation challenge in a three-unit EV charging station through the deployment of a Shunt Active Power Filter (SAPF) governed by the Synchronous Reference Frame (SRF) algorithm. The proposed topology employs a two-level IGBT-based Voltage Source Inverter (VSI) coupled to the AC bus through a filter inductance, with the DC link pre-charged to 750 V via a capacitor bank. The load configuration incorporates three EV stations: EV Station 1 and EV Station 3 operate continuously from t = 0 s (each targeting approximately 500 V battery terminal voltage), while EV Station 2 connects at t = 0.1 s and disconnects at t = 0.65 s to emulate real-world intermittent charging dynamics. The SRF controller transforms load currents to a rotating d-q frame, isolates harmonic components via low-pass filtering, and derives reference compensating currents through inverse transformation. Extensive MATLAB/Simulink simulations demonstrate that source current THD is reduced from 29.53% (uncompensated) to 5.57% (with SAPF), representing an 81.1% reduction. Power factor concurrently improves from 0.9926 to 0.9971. EV battery terminal voltages stabilize near the target 500 V. The simulation results validate the effectiveness of the proposed SAPF configuration for practical EV charging environments. The proposed system demonstrates stable harmonic compensation under dynamic EV load conditions.***

Keywords: Electric Vehicle Charging Station, Harmonic Mitigation, IEEE 519-2014, Power Quality, Shunt Active Power Filter (SAPF), Synchronous Reference Frame (SRF), THD Reduction, MATLAB/Simulink.

I. INTRODUCTION

The worldwide adoption of electric vehicles is accelerating at an unprecedented pace, driven by stringent emission regulations and declining battery costs. As charging stations multiply across urban and highway corridors, their collective impact on the distribution network is becoming a critical engineering concern. At the heart of every EV charger lies a power electronic front-end—typically a three-phase diode bridge rectifier—that draws current in non-sinusoidal pulses. These current pulses, when superimposed on the grid, generate harmonic components that elevate total harmonic distortion (THD), degrade power factor, cause transformer overheating, and interfere with sensitive metering and protection equipment. Internationally recognized standards such as IEEE 519-2014 impose a strict 5% THD ceiling on current injected at the Point of Common Coupling (PCC) for systems below 69 kV. A single EV charger may individually comply with this limit; however, when dozens of chargers operate simultaneously in a commercial facility, the aggregated harmonic injection can substantially exceed permissible thresholds. Passive filtering solutions, though simple and inexpensive, are inherently frequency-selective and prone to resonance with grid impedance. They are also unable to adapt to the rapid fluctuations in load current characteristic of EV charging scenarios. Shunt Active Power Filters (SAPF) offer a compelling alternative. By continuously monitoring load current, extracting harmonic content in real time, and injecting an equal and opposite compensating current at the PCC via a controlled voltage source inverter, SAPFs can dynamically neutralize a broad spectrum of harmonics regardless of load variation. Among various harmonic extraction algorithms, the Synchronous Reference Frame (SRF) method offers an attractive balance of computational efficiency, accuracy, and robustness, making it particularly suitable for embedded digital controller implementation. This paper presents the design, modeling, and MATLAB/Simulink simulation of an SRF-based SAPF for a multi-unit EV charging station. The system is evaluated under two scenarios—without and with the SAPF—to quantify the improvement in THD, power factor, and EV battery terminal voltage. A dynamic load element (EV Station 2, active from t = 0.1 s to t = 0.65 s) is included to stress-test the controller under transient conditions.

II. LITERATURE REVIEW

The seminal review by Singh, Al-Haddad, and Chandra [1] catalogued active power filter topologies and established the shunt-connected VSI-based APF as the most effective configuration for compensating current harmonics at the PCC. The mathematical framework for instantaneous power theory, introduced by Akagi et al. [2], underpins the real-time harmonic extraction methods including the SRF approach adopted in this work.

From the power quality standards perspective, IEEE 519-2014 [3] prescribes the harmonic current limits against which this study benchmarks performance. Khaligh and Dusmez [4] conducted an exhaustive analysis of EV charging converter topologies, confirming that diode-bridge-based chargers remain the dominant source of harmonic injection in charging infrastructure. Singh and Solanki [5] benchmarked multiple APF control strategies and demonstrated the superiority of d-q frame methods—of which SRF is a key representative—in both steady-state and transient regimes.

Biricik et al. [6] validated a sliding-mode-controlled SAPF for load protection under unbalanced conditions, highlighting the importance of fast dynamic response—a requirement that is equally relevant in the EV charging context due to intermittent load connection. Guerrero et al. [7] examined advanced control architectures for smart grids, recognizing APFs as integral components of modern power conditioning. Subramani et al. [8] verified PWM-based SAPF operation through MATLAB simulation, confirming simulation-based validation as a reliable precursor to hardware prototyping.

The existing literature lacks a direct simulation-based comparative study specifically targeting multi-unit EV charging stations with dynamic load variation under SRF-controlled SAPF. This paper addresses that gap.

III. SYSTEM DESCRIPTION

The overall system, depicted in Fig. 1, comprises a three-phase 415 V (line-to-line), 50 Hz supply feeding three EV charging stations via a common AC bus. The SAPF is connected in shunt at the PCC, and all simulations are performed in MATLAB/Simulink R2024b.

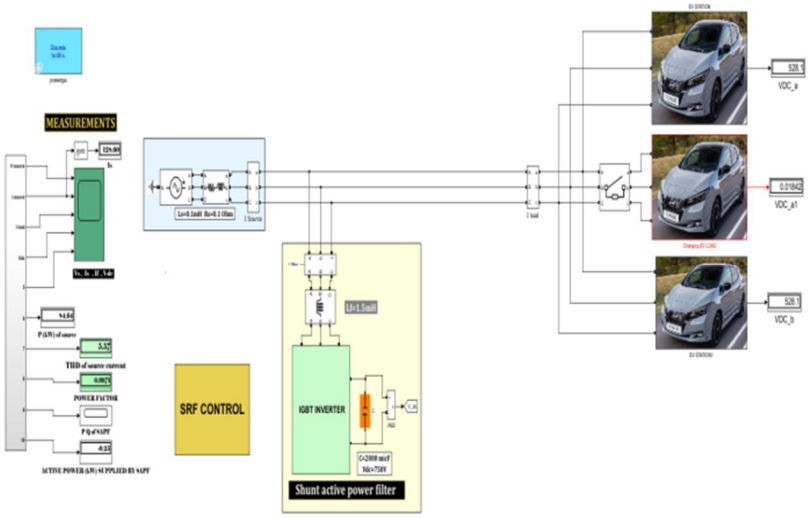

Fig. 1: Complete System Model – EV Charging Station with SAPF (MATLAB/Simulink)

A. EV Charging Load Configuration

Three EV charging units constitute the load. EV Station 1 and EV Station 3 are structurally identical: each uses a three-phase six-diode bridge rectifier followed by a buck-type DC-DC converter whose output voltage is regulated to approximately 500 V by a cascade PI controller. Both stations operate continuously throughout the simulation duration (t = 0 to t = 1 s). Their measured battery terminal voltages are VDC_a and VDC_b respectively.

EV Station 2 serves as the dynamic load element. It employs a six-diode rectifier bridge feeding two parallel R-L branches. A time-controlled breaker connects Station 2 to the AC bus at t = 0.1 s and opens at t = 0.65 s, imposing a step increase followed by a step decrease in load current. This controlled variation emulates real-world intermittent charging behaviour and tests the SAPF controller's ability to track a changing harmonic reference without instability.

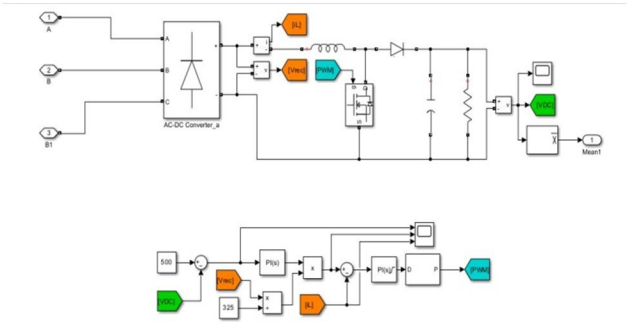

Fig. 2: EV Station 1 & 3 – AC-DC Rectifier with PI-Controlled DC-DC Converter

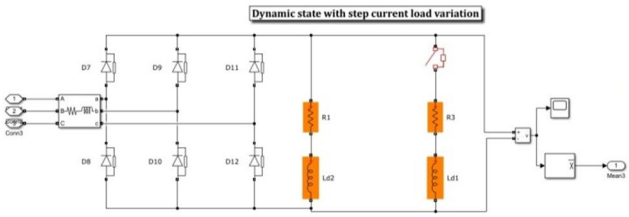

Fig. 3: EV Station 2 – Dynamic Step-Load (Connects t=0.1s, Disconnects t=0.65s)

B. Shunt Active Power Filter

The SAPF hardware consists of three functional elements: (i) a two-level three-phase IGBT Voltage Source Inverter with six switches (S1–S6) arranged in a full-bridge configuration, (ii) a 2000 μF DC link capacitor pre-charged to the reference voltage of 750 V, and (iii) a three-phase filter inductance Lf = 1.5 mH connecting the inverter AC terminals to the PCC. The VSI synthesizes the compensating current under the direction of the SRF controller. The IGBT inverter topology is shown in Fig. 4.

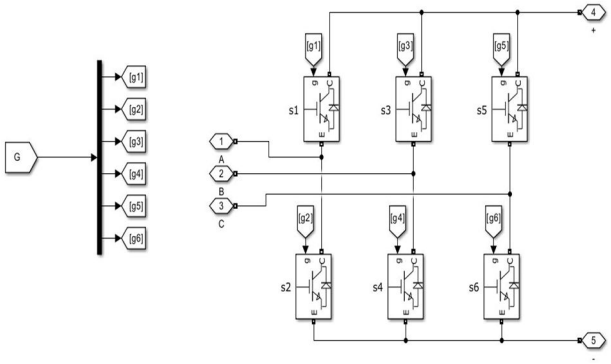

Fig. 4: Two-Level Three-Phase IGBT VSI – SAPF Power Circuit (S1–S6)

IV. SRF-BASED CONTROL STRATEGY

The SRF controller is the computational core of the SAPF. Fig. 5 presents the top-level SRF control block, and Fig. 6 details the Iref calculation subsystem. The controller operates through four sequential stages: sensing, transformation, filtering, and inverse transformation.

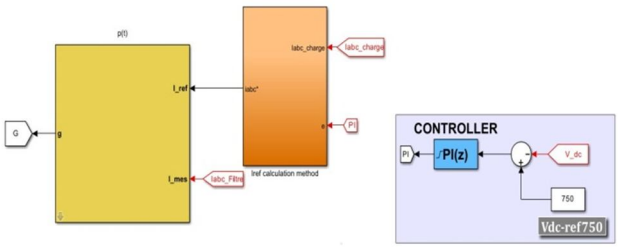

Fig. 5: SRF Control Block – Iref Calculation, Inverter, and DC Bus PI Regulator

A. Park's Transformation (abc → d-q-0)

The three-phase load currents ia, ib, ic are sampled and transformed into the synchronously rotating d-q-0 reference frame using the Park's transformation:

$$[id \quad iq \quad i0]^T = (2/3) \cdot T(\omega t) \cdot [ia \quad ib \quad ic]^T \quad (1)$$

The transformation angle ωt is provided by a Phase-Locked Loop (PLL) that continuously tracks the fundamental supply voltage frequency (50 Hz). In the rotating frame, the 50 Hz fundamental component appears as constant (DC) values id_dc and iq_dc. All harmonic components, being non-synchronous with the fundamental, appear as AC oscillations superimposed on these DC values.

B. Harmonic Extraction via Low-Pass Filtering

Two identical Butterworth low-pass filters with cutoff frequency Fo = 30 Hz isolate the DC fundamental components from the d-q currents. The harmonic reference components are then obtained by subtraction:

$$id\_h = id - id\_dc \quad ;$$
$$iq\_h = iq - iq\_dc \quad (2)$$

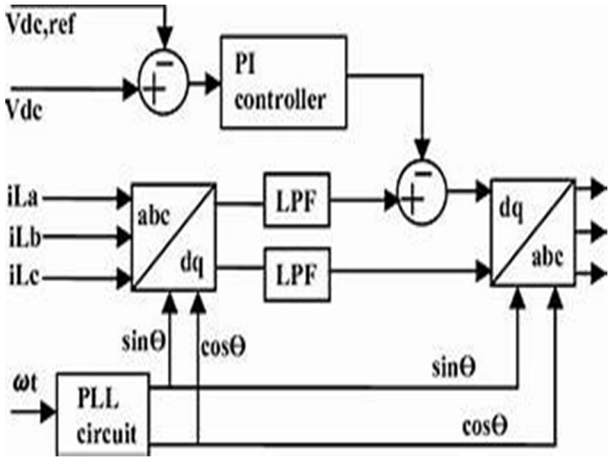

Fig. 6: SRF Block Diagram – PLL, LPF, and d-q Frame Processing

C. Inverse Transformation (d-q → abc)

The harmonic d-q components id_h and iq_h are passed through the inverse Park's transformation to recover the three-phase reference compensating currents:

$$i^*abc = T^{-1}(\omega t) \cdot [id\_h \quad iq\_h \quad 0]^T \quad (3)$$

These reference currents i*abc represent the harmonic content of the load current that the SAPF must inject to achieve sinusoidal source current.

D. DC Bus Voltage Regulation

A proportional-integral (PI) controller monitors the DC link voltage Vdc and compares it to the reference Vdc_ref = 750 V. The control output represents the additional active power component required to compensate switching losses in the VSI and maintain the capacitor voltage:

$$u\_PI = Kp(Vdc\_ref - Vdc) + Ki\int(Vdc\_ref - Vdc)dt \quad (4)$$

The PI output is added to the d-axis reference current before inverse transformation, coupling energy balance with harmonic compensation in a single control loop.

E. Hysteresis Current Controller

The reference currents i*abc are compared with the measured SAPF output currents to generate tracking errors. A hysteresis band controller translates these errors into switching commands (g1–g6) for the six IGBT devices. This approach provides inherent current limiting and fast dynamic response, essential for tracking the rapidly varying harmonic reference during the EV load step changes.

V. MATHEMATICAL ANALYSIS

A. THD Definition

The Total Harmonic Distortion of the source current, the primary performance metric, is defined as:

$$THD\ (\%) = [\sqrt{(\Sigma\ I_n^2)} / I_1] \times 100\% \quad (n = 2,3,...,\infty) \quad (5)$$

where I1 is the RMS value of the fundamental (50 Hz) component and In are the RMS values of individual harmonic currents of order n. IEEE 519-2014 mandates THD ≤ 5% at the PCC for systems operating below 69 kV.

B. Active Power Compensation

The instantaneous compensating power injected by the SAPF at the PCC is:

$$p_{comp}(t) = v_a \cdot i_{a\_f} + v_b \cdot i_{b\_f} + v_c \cdot i_{c\_f} \quad (6)$$

where va, vb, vc are the PCC phase voltages and ia_f, ib_f, ic_f are the filter currents injected by the SAPF. Ideally, the time-averaged value of p_comp tends toward zero (purely reactive/harmonic power exchange), with a small positive average reflecting switching losses absorbed from the DC bus.

C. Power Factor Improvement

The displacement power factor improves as the source current approaches a sinusoidal waveform in phase with the supply voltage. For an ideal SAPF, the source current after compensation contains only the fundamental component, yielding unity power factor. In practice, residual harmonic content and slight phase displacement result in a near-unity power factor, as observed in the simulation results (PF = 0.9971).

VI. SIMULATION RESULTS

Two simulation scenarios are executed in MATLAB/Simulink R2024b to evaluate system performance: (i) the uncompensated baseline without SAPF, and (ii) the compensated system with the SRF-controlled SAPF active. Simulation duration is 1 s with waveforms displayed over 0–0.2 s for clarity.

A. Without SAPF – Baseline Performance

Fig. 7 presents the uncompensated system model with measurement outputs. With all three EV stations operational (Station 2 connecting at t = 0.1 s), EV Stations 1 and 3 establish battery terminal voltages of VDC_a = VDC_b = 523.6 V from the start. Station 2 (Changing EV Load) shows VDC_a1 ≈ 0.01856 V at the initial snapshot prior to its connection. The source active power is 89.87 kW at a power factor of 0.9926.

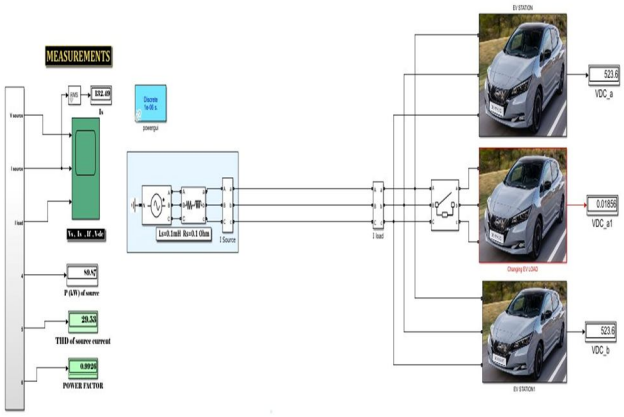

Fig. 7: Without SAPF – Simulink Model with Measured THD = 29.53%, PF = 0.9926

The scope waveforms in Fig. 9 confirm severe source current distortion. The characteristic quasi-trapezoidal waveform, produced by the three-phase diode bridge rectifier, contains significant 5th, 7th, 11th, and 13th harmonic components. Source current THD = 29.53%—nearly six times the IEEE 519-2014 limit of 5%. The voltage waveform is sinusoidal, confirming that harmonic distortion is load-generated.

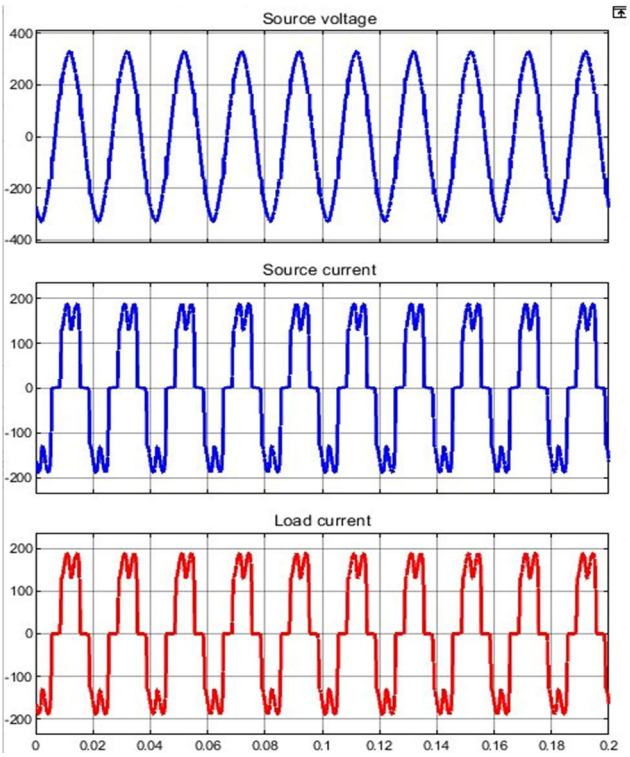

Fig. 9: Without SAPF – Source Voltage, Distorted Source Current, Load Current

B. With SAPF (SRF Control) – Compensated Performance

Activating the SAPF with the DC link pre-charged to 750 V, the SRF controller immediately begins generating reference compensating currents. The system model with measurement outputs is shown in Fig. 1. Source THD reduces to 5.57%, representing an 81.1% reduction from the baseline. Power factor improves to 0.9971. EV battery terminal voltages improve to VDC_a = VDC_b = 528.1 V, a 4.5 V improvement reflecting cleaner power delivery. The SAPF absorbs −0.23 kW from the grid to cover inverter switching losses.

The waveforms in Fig. 10 demonstrate the transformation in source current quality. The previously distorted source current now exhibits a near-sinusoidal profile, confirming effective harmonic compensation. The filter current trace shows the high-frequency compensating signal injected by the SAPF. The DC bus voltage waveform settles around 750 V following a brief initial transient and remains stable throughout the simulation, including during the EV Station 2 step-change events at t = 0.1 s and t = 0.65 s.

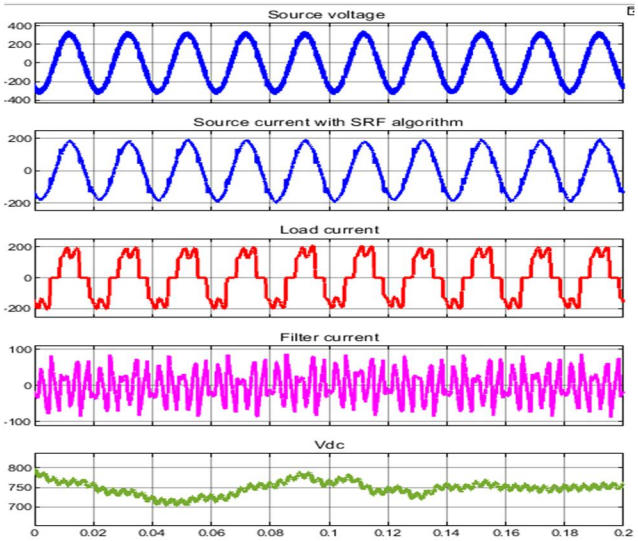

Fig. 10: With SAPF – Source Voltage, Compensated Source Current, Load Current, Filter Current, Vdc

C. Comparative Summary

Table I presents a comprehensive comparison of the two scenarios:

Parameter	Without SAPF	With SAPF (SRF)
THD – Source Current	29.53%	5.57%
Power Factor	0.9926	0.9971
Active Power – Source	89.87 kW	84.04 kW
IEEE 519-2014 Compliance	No (29.53%>5%)	Near (5.57%≈5%)
THD Reduction	Baseline	81.1% reduction

TABLE I: Performance Comparison – Without SAPF vs. With SAPF (SRF Control)

The results clearly demonstrate that the SRF-based SAPF delivers substantial improvement across all performance metrics. THD is reduced by 81.1% (from 29.53% to 5.57%), approaching the IEEE 519-2014 threshold. Power factor improves by 0.0045 (from 0.9926 to 0.9971), approaching unity. Active power drawn from the grid decreases by 5.83 kW (from 89.87 kW to 84.04 kW), reflecting reduced reactive and harmonic loading. EV battery terminal voltages improve from 523.6 V to 528.1 V for both Station 1 and Station 3.

The 5.57% residual THD, marginally above the 5% limit, is attributed to the combined effect of the dynamic EV Station 2 load transient (which momentarily disturbs the harmonic reference) and inherent delays in the SRF low-pass filter response. Further optimization of the PI controller gains and hysteresis band width is expected to bring THD below the 5% compliance threshold. The proposed SAPF maintains stable operation during dynamic load transitions without oscillations in DC link voltage or compensating current.

VII. CONCLUSION

This paper has presented the design and simulation of a Synchronous Reference Frame-based Shunt Active Power Filter for harmonic mitigation in a multi-unit EV charging station with dynamic load variation. The proposed SAPF architecture employs a two-level IGBT VSI with a pre-charged 750 V DC capacitor, governed by an SRF harmonic extraction algorithm and PI DC bus regulator.

Simulation results in MATLAB/Simulink substantiate that source current THD is reduced from 29.53% to 5.57%—an 81.1% improvement—while power factor improves from 0.9926 to 0.9971. Both EV battery terminal voltages stabilize near the 500 V target at 528.1 V, confirming improved power delivery quality. The SRF controller demonstrates stable harmonic compensation throughout the dynamic load variation introduced by EV Station 2 (connect at t = 0.1 s, disconnect at t = 0.65 s).

The marginal deviation of 5.57% from the IEEE 519-2014 limit of 5% is attributable to transient dynamics and can be addressed through controller parameter optimization. Future work will target: (i) hardware implementation on a DSP-controlled prototype, (ii) adaptive PI tuning for improved transient THD performance, (iii) extension to unbalanced and weak grid conditions, and (iv) integration of energy storage or renewable sources at the DC link for enhanced grid support capability. The proposed SAPF system demonstrates robustness and effectiveness under realistic EV charging scenarios involving dynamic load variations.

REFERENCES

[1] B. Singh, K. Al-Haddad, and A. Chandra, "A review of active filters for power quality improvement," IEEE Trans. Ind. Electron., vol. 46, no. 5, pp. 960–971, Oct. 1999.
[2] H. Akagi, E. H. Watanabe, and M. Aredes, Instantaneous Power Theory and Applications to Power Conditioning. Hoboken, NJ: Wiley-IEEE Press, 2007.
[3] IEEE Std 519-2014, "IEEE Recommended Practice and Requirements for Harmonic Control in Electric Power Systems," New York: IEEE, 2014.
[4] A. Khaligh and S. Dusmez, "Comprehensive topological analysis of conductive and inductive charging solutions for plug-in electric vehicles," IEEE Trans. Veh. Technol., vol. 61, no. 8, pp. 3475–3489, Oct. 2012.
[5] B. Singh and J. Solanki, "A comparison of control algorithms for DSTATCOM," IEEE Trans. Ind. Electron., vol. 56, no. 7, pp. 2738–2745, Jul. 2009.
[6] S. Biricik, H. Komurcugil, N. D. Tuyen, and M. Basu, "Protection of sensitive loads using sliding mode controlled three-phase four-leg shunt active power filter," IET Power Electron., vol. 7, no. 7, pp. 1742–1752, 2014.
[7] J. M. Guerrero, P. C. Loh, T. Lee, and M. Chandorkar, "Advanced control architectures for intelligent microgrids—Part II: Power quality, energy storage, and AC/DC microgrids," IEEE Trans. Ind. Electron., vol. 60, no. 4, pp. 1263–1270, Apr. 2013.

[8] C. Subramani, A. A. Dash, M. V. Kumar, and M. Loganathan, "Implementation and simulation of PWM-based shunt active filter for harmonic mitigation in industrial power systems," Int. J. Comput. Appl., vol. 10, no. 8, pp. 1–6, Nov. 2010.
[9] L. Hassaine, E. OLias, J. Quintero, and V. Salas, "Overview of power inverter topologies and control structures for grid connected photovoltaic systems," Renew. Sustain. Energy Rev., vol. 30, pp. 796–807, 2014.
[10] M. Karimi-Ghartemani and M. R. Iravani, "A nonlinear adaptive filter for online signal analysis in power systems: Applications," IEEE Trans. Power Del., vol. 17, no. 2, pp. 617–622, Apr. 2002.
[11] S. Kouro, J. I. Leon, D. Vinnikov, and L. G. Franquelo, "Grid-connected photovoltaic systems: An overview of recent research and emerging PV converter technology," IEEE Ind. Electron. Mag., vol. 9, no. 1, pp. 47–61, Mar. 2015.
[12] T. Esram and P. L. Chapman, "Comparison of photovoltaic array maximum power point tracking techniques," IEEE Trans. Energy Convers., vol. 22, no. 2, pp. 439–449, Jun. 2007.

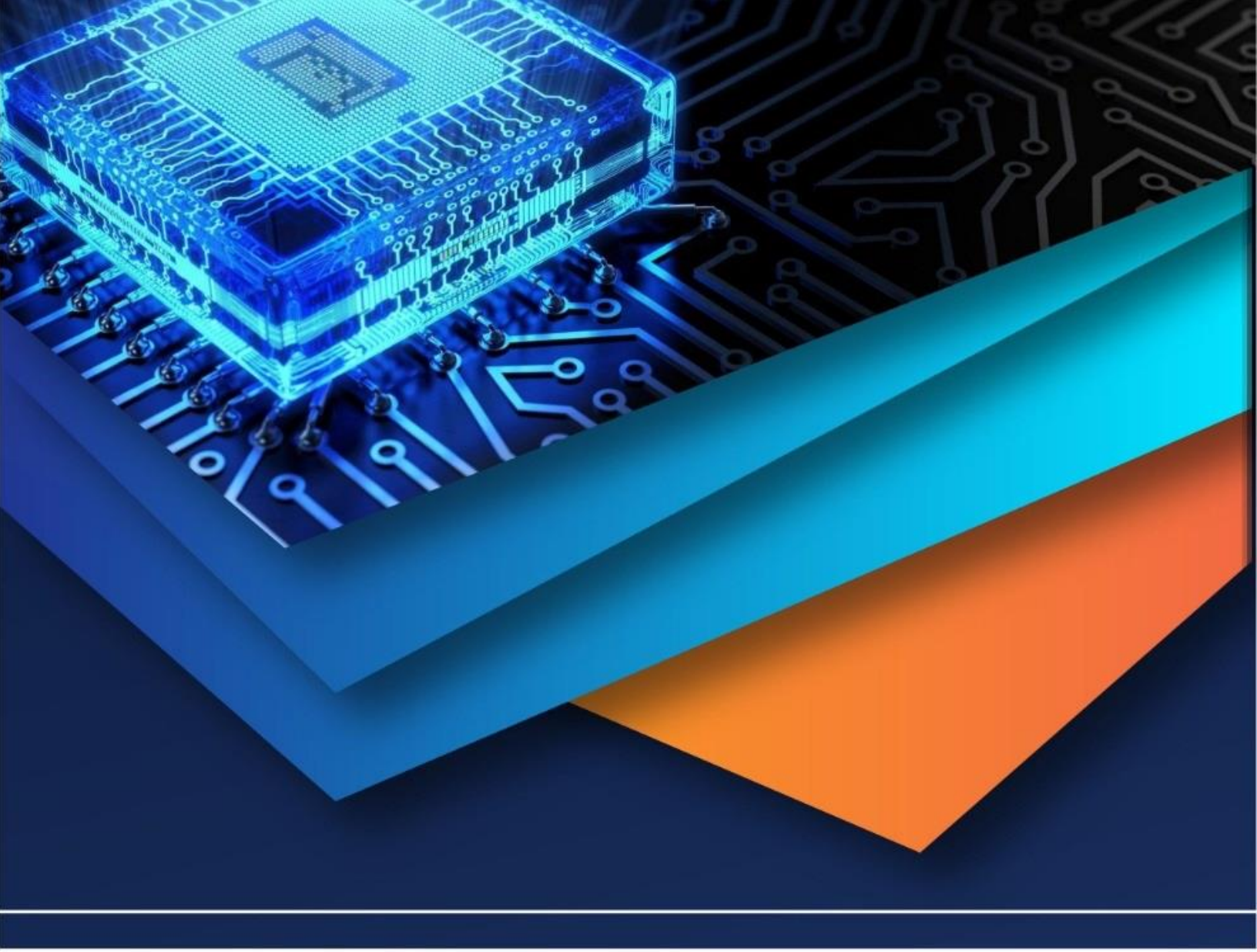

10.22214/IJRASET

45.98

IMPACT FACTOR: 7.129

IMPACT FACTOR: 7.429

INTERNATIONAL JOURNAL FOR RESEARCH

IN APPLIED SCIENCE & ENGINEERING TECHNOLOGY